Lecture 1

El Nino - Southern Oscillations: Phenomenology and dynamical background

Eli Tziperman

1.1 A brief description of the phenomenology

1.1.1 The mean state

Consider first a few of the main elements of the mean state of the equatorial Pacific ocean and atmosphere that play a role in ENSO's dynamics. For a more comprehensive introduction to the observed phenomenology see [47]; many useful pictures and animations are available on the El Nino theme page at http://www.pmel.noaa.gov/tao/elnino/nino-home.html.

The mean winds are easterly and clearly show the Inter-Tropical Convergence Zone (ITCZ) just north of the equator (Fig. 11); a vertical schematic section shows the Walker circulation (Fig. 12) with air rising over the "warm pool" area of the West Pacific and sinking over the East Pacific. The seasonal motion of the ITCZ and the modulation of the Walker circulation by the ENSO events are key players in ENSO's dynamics as will be seen below.

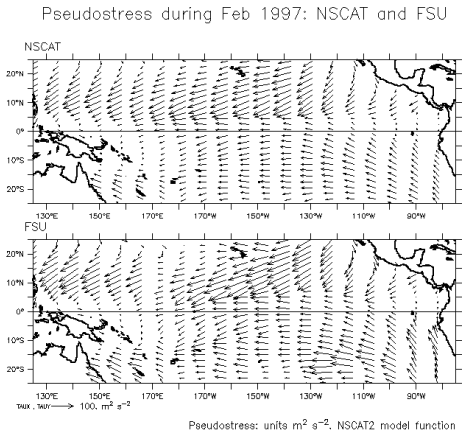

Figure 11: The wind stress showing the ITCZ in Feb 1997, using two different data sets (http://-www.pmel.noaa.gov/~kessler/nscat/vector-comparison-feb97.gif).

The mean easterly wind stress causes the above-thermocline warm water to accumulate in the West Pacific, causing the thermocline to slope as shown in the upper panel of Fig. 13. The thermocline slope induces an east-west gradient in the sea surface temperature (SST), creating the "cold tongue" in the east equatorial Pacific and the "warm pool" on the west (Fig. 14). This gradient, in turn, affects the Walker circulation and the mean wind stress as mentioned above.

1.1.2 ENSO variability

We now proceed to a brief description of the phenomenology of the ENSO variability about the mean climatology described above. The spatial structure of SST anomalies during La Nina, normal conditions and during El Nino are shown in Fig. 15. The slope in the equatorial thermocline varies quite dramatically between the El Nino, La Nina and normal conditions (Fig. 16).

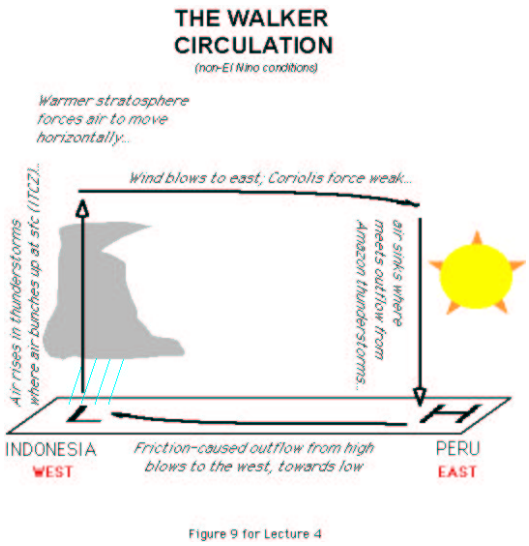

Figure 12: The Walker circulation (http://www.ldeo.columbia.edu/dees/ees/climate/slides/complete_index.html).

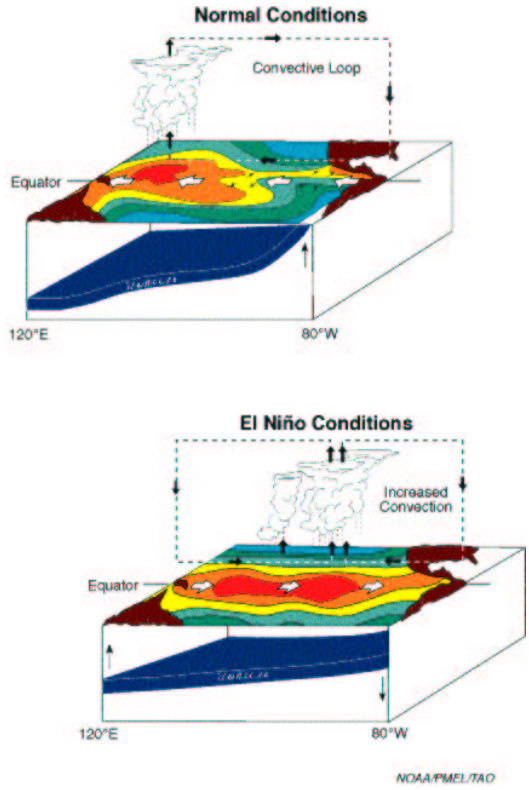

Figure 13: Schematic plot showing the equatorial thermocline slope during normal and El Nino conditions from the El Nino theme page http://www.pmel.noaa.gov/toga-tao/el-nino/.

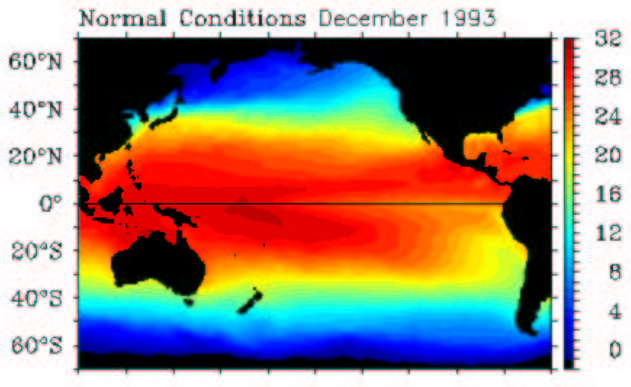

Figure 14: Normal SST conditions in the equatorial Pacific, showing the warm pool in the west and the cold tongue in the east (Reynolds data, from El Nino Theme page).

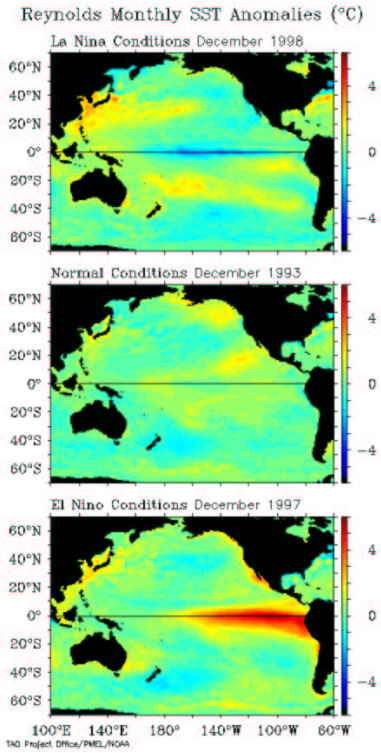

Figure 15: The anomalous SST field during typical La Nina, normal conditions and El Nino.

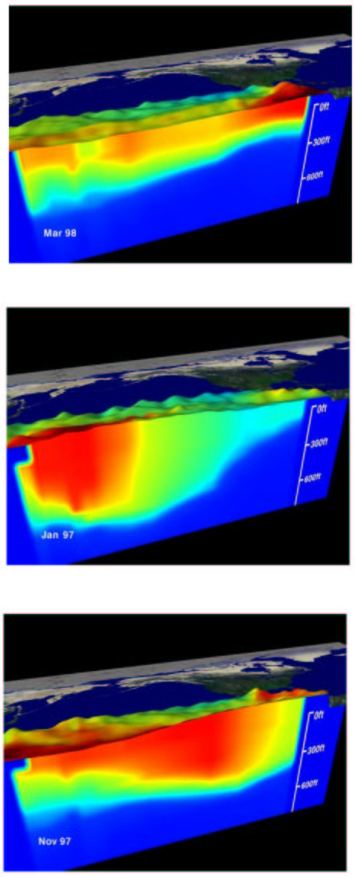

Figure 16: An east-west vertical section along the equatorial thermocline during normal, La Nina and El Nino conditions, from El Nino theme page http://www.pmel.noaa.gov/tao/elnino/nino-home.html.

The SST changes shown above during the ENSO cycle are accompanied by wind anomalies that cause the mean easterlies to weaken during El Nino events and strengthen during La Nina events. In order to obtain some feeling for the structure of the evolution in time during ENSO events, consider the equatorial SST as function of longitude and time, shown in Fig. 17. One can see the several-year time scale between El Nino events, and the irregular amplitude and time separation between the events. Also, note that El Nino events tend to reach their peak toward the end of the calendar year. For the implications of ENSO events on global weather etc see, for example, http://www.pmel.noaa.gov/toga-tao/el-nino/impacts.html. The purpose of the toy models to be considered below would be to explain the coupled ocean-atmosphere variability in the winds, thermocline slope and SST, as well as the time scale, the aperiodicity, and locking to the seasonal cycle of these events.

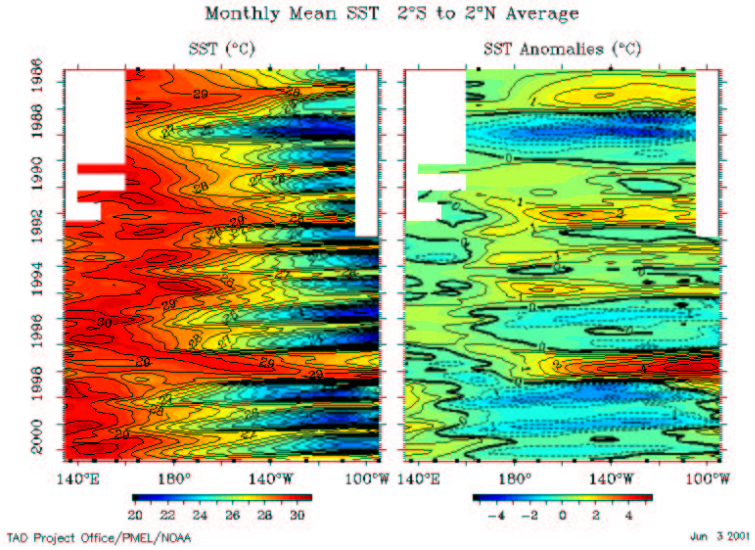

Figure 17: SST along the Equatorial Pacific as a Hovemoller diagram (plotted as function of longitude and time), for both the full SST and anomalies with respect to climatology. From El Nino theme page http://www.pmel.noaa.gov/toga-tao/el-nino/

1.1.3 Main issues

To summarize, the main questions to be addressed below regarding ENSO's dynamics using various conceptual models are

1. What is the mechanism of the El Nino cycle?
2. Why is the mean period quite robustly 4 years?
3. Is ENSO self-sustained or is it damped and requires external forcing by weather noise for example in order to be excited?
4. Why are ENSO events irregular: is it due to chaos? noise?
5. Why do ENSO events tend to peak toward the end of the calendar year (phase locking to the seasonal cycle)?

1.2 A brief equatorial dynamics background

1.2.1 Importance of thermocline dynamics and reduced gravity models

The phenomenology above indicates that motions of the equatorial thermocline are critical to ENSO's dynamics. We therefore start by deriving the simplest equations that describe the thermocline dynamics. Consider a two layer model, with the lower layer much thicker and thus assumed to be at rest (Fig. 18).

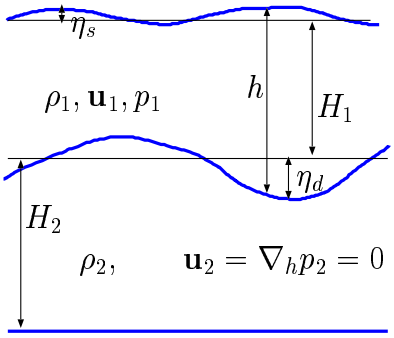

Figure 18: The $1\frac{1}{2}$ layer model

The momentum equations (Boussinesq approximation)

$$\frac{\partial \mathbf{u}}{\partial t} + \mathbf{u}\cdot\nabla\mathbf{u} + 2\Omega\times\mathbf{u} = -\frac{1}{\rho_0}\nabla p + \mathbf{g}\rho/\rho_0 + \nu\nabla^2\mathbf{u}$$

then imply that because the horizontal velocity in the lower layer is zero, $\mathbf{u}_{2H} = (u_2, v_2) = 0$, the horizontal pressure gradients are also zero in the lower layer, $\nabla_H p_2 = 0$, with $\nabla_H = (\frac{\partial}{\partial x}, \frac{\partial}{\partial y})$ being the two dimensional horizontal gradient, and where ∇ above stands for the three dimensional gradient operator. Assuming a hydrostatic vertical momentum balance (because $H \ll L$)

$$p_z = -g\rho$$

and integrating this balance in z, we can write the pressure at a depth z in the upper layer as

$$p_1(x,y,z,t) = g(-z+\eta_s(x,y,t))\rho_1$$

so that

$$-\frac{1}{\rho_0}\nabla p_1 \approx -g\nabla\eta_s.$$

In the lower layer, the pressure is

$$p_2(x,y,z,t) = g(H_1+\eta_s-\eta_d)\rho_1 + g(H_2+\eta_d-z)\rho_2$$

so that

$$\begin{aligned}\frac{1}{\rho_0}\nabla_H p_2 &= \nabla_H\left(\frac{\rho_1}{\rho_0}g\eta_s + \frac{\rho_2-\rho_1}{\rho_0}g\eta_d\right)\\ &\approx \nabla_H(g\eta_s + g'\eta_d)\end{aligned}$$

where $g' \equiv \frac{\rho_2-\rho_1}{\rho_0}g \approx \frac{\rho_2-\rho_1}{\rho_2}g$. That this deep horizontal pressure gradient vanishes gives

$$g\nabla_H\eta_s = -g'\nabla_H\eta_d$$

which, together with the observation that $g' \ll g$ so that $\eta_s \ll \eta_d$, implies

$$g\nabla_H \eta_s = -g'\nabla_H \eta_d \approx g'\nabla_H h.$$

Together with the above relations this finally allows us to write the horizontal pressure gradient in the upper layer as a function of the upper layer thickness

$$-\frac{1}{\rho_0}\nabla p_1 = -g'\nabla h.$$

1.2.2 The equatorial β plane

The objective now is to find a convenient representation of the effect of the earth rotation near the equator [43, 20]. We start with horizontal momentum equations for a $1\frac{1}{2}$ layer fluid as above, on a sphere, where we use

$$2\vec{\Omega}\times\mathbf{u} = 2\Omega\begin{pmatrix} w\cos\theta - v\sin\theta \\ u\sin\theta \\ -u\cos\theta \end{pmatrix}.$$

to find

$$\begin{aligned} \frac{du}{dt} + \frac{uw}{r} - \frac{uv}{r}\tan\theta + 2\Omega(w\cos\theta - v\sin\theta) &= -\frac{g'}{r\cos\theta}\frac{\partial h}{\partial\phi} + \mathcal{F}_\phi \\ \frac{dv}{dt} + \frac{wv}{r} - \frac{u^2}{r}\tan\theta + 2\Omega u\sin\theta &= -\frac{g'}{r}\frac{\partial h}{\partial\theta} + \mathcal{F}_\theta \end{aligned}$$

where

$$\frac{d}{dt} \equiv \frac{\partial}{\partial t} + \frac{u}{r\cos\theta}\frac{\partial}{\partial\phi} + \frac{v}{r}\frac{\partial}{\partial\theta} + w\frac{\partial}{\partial r},$$

and where $(\mathcal{F}_\phi, \mathcal{F}_\theta)$ represent the forcing and dissipation terms, and θ, ϕ the latitude and longitude. Next, assume linear momentum dynamics, and use the fact that $w \ll (u,v)$. Also, write the vertical coordinate as $r = r_0 + z$ where r_0 is the earth radius, so that within a thin layer of fluid (ocean thickness $\ll$ earth radius) we have $1/r = 1/(r_0+z) \approx 1/r_0$, and therefore,

$$\begin{aligned} \frac{\partial u}{\partial t} - 2\Omega\sin\theta v &= -\frac{g'}{r_0\cos\theta}\frac{\partial h}{\partial\phi} + \mathcal{F}_\phi \\ \frac{\partial v}{\partial t} + 2\Omega\sin\theta u &= -\frac{g'}{r_0}\frac{\partial h}{\partial\theta} + \mathcal{F}_\theta. \end{aligned}$$

Next, we restrict our attention to near-equatorial regions, where we can define local Cartesian coordinates around some central location (θ_0, ϕ_0)

$$\begin{aligned} x &\equiv r_0\cos\theta_0(\phi - \phi_0) \\ y &\equiv r_0(\theta - \theta_0), \end{aligned}$$

as well as expand the Coriolis force as

$$\begin{aligned} 2\Omega\sin\theta &\approx 2\Omega\sin\theta_0 + 2\Omega\cos\theta_0(\theta - \theta_0) \\ &= f_0 + \beta y \end{aligned}$$

with $\beta \equiv 2\Omega\cos\theta_0/r_0$. An expansion around the equator $\theta_0 = 0$ leads to $f_0 = 0$. Using a simple linear friction law and incorporating the wind stress forcing

$$\begin{aligned} \mathcal{F}_\phi &= \mathcal{F}_x = -\varepsilon u + \tau^x/(\rho_0 H) \\ \mathcal{F}_\theta &= \mathcal{F}_y = -\varepsilon v + \tau^y/(\rho_0 H) \end{aligned}$$

we obtain the final set of β-plane momentum equations for a $1\frac{1}{2}$ layer model

$$\frac{\partial u}{\partial t} - \beta y v = -g' \frac{\partial h}{\partial x} - \varepsilon u + \frac{\tau^x}{\rho_0 H} \quad (1)$$

$$\frac{\partial v}{\partial t} + \beta y u = -g' \frac{\partial h}{\partial y} - \varepsilon v + \frac{\tau^y}{\rho_0 H}. \quad (2)$$

and with three unknowns (u, v, h) we need a third equation which is provided by the linearized mass conservation equation (which also includes on the rhs a rough linear parameterization of entrainment (mixing) at the base of the water layer above the thermocline)

$$\frac{\partial h}{\partial t} + H\left(\frac{\partial u}{\partial x} + \frac{\partial v}{\partial y}\right) = -\varepsilon h. \quad (3)$$

1.2.3 Equatorial waves

The derivation here follows Gill [20]. Consider first the case of an equatorial Kelvin wave, which is a special solution of (1,2,3) for the case of zero meridional velocity ($v = 0$), no forcing and no dissipation. In this case, these equations reduce to

$$\begin{aligned} \frac{\partial u}{\partial t} &= -g' \frac{\partial h}{\partial x} \\ \beta y u &= -g' \frac{\partial h}{\partial y} \\ \frac{\partial h}{\partial t} + H \frac{\partial u}{\partial x} &= 0 \end{aligned}$$

Note the geostrophic balance in the y-momentum equation. Substituting $e^{i(kx-\omega t)}$ dependence for all three variables, we get from the first that $u = (kg'/\omega)h$, so that the third one gives the dispersion relation

$$\omega^2 = (g'H)k^2$$

which is the dispersion relation of a simple shallow water gravity wave. The second equation then gives $\beta y \frac{kg'}{\omega} h = -g' \frac{\partial h}{\partial y}$, or

$$\frac{\partial h}{\partial y} = -\frac{\beta k}{\omega} y h.$$

We are searching for equatorial-trapped solutions, and we note that the solution for the y-structure decays away from the equator only when $k > 0$. This implies that the wave solution we have found must be eastward propagating! Using the dispersion relation, with

$$c \equiv \sqrt{g'H} \approx (9.8 \times 10^2 * cm\, sec^{-2} \times 5 * 10^{-3} \times 100 \times 10^2 cm)^{1/2} \approx 2.2 m/sec$$

we finally have

$$h_{Kelvin}(x, y, t) \propto e^{-\frac{1}{2}(\beta/c)y^2} e^{i(kx-\omega t)}.$$

Note that the decay scale away from the equator is the equatorial Rossby radius of deformation defined as

$$L_{eq}^R \equiv \sqrt{c/2\beta} \approx (c/(2 \times 2.3 \times 10^{-11} m^{-1} sec^{-1}))^{1/2} \approx 220 km$$

Next is the derivation of the full set of equatorial waves, where we now do not assume that the meridional velocity v vanishes. Substitute $h(x,y,t) = h(y)e^{i(kx-\omega t)}$ dependence, and similarly for (u,v), and derive a single equation for h to find the parabolic cylinder equation (Gill, [20], section 11.6.1)

$$\frac{d^2v}{dy^2} + \left(\frac{\omega^2}{c^2} - k^2 - \frac{\beta k}{\omega} - \frac{\beta^2}{c^2}y^2\right)v = 0.$$

The solutions that vanish at $y \to \pm\infty$ occur only for certain relations between the coefficients, and these relations serve as the dispersion relation

$$\frac{\omega^2}{c^2} - k^2 - \frac{\beta k}{\omega} = (2n+1)\frac{\beta}{c}. \tag{4}$$

Note that the Kelvin wave dispersion relation is formally a solution of this dispersion relation for $n = -1$ (simply check that $\omega = ck$ satisfies (4) for $n = -1$). The meridional structure of the waves in this case of equatorially trapped solutions is expressed in terms of the Hermit polynomials

$$v = 2^{-n/2}H_n((\beta/c)^{1/2}y)\exp(-\beta y^2/2c)\cos(kx-\omega t)$$

and is shown in Fig. 19, where

$$H_0 = 1; \qquad H_1 = 2x; \qquad H_2 = 4x^2 - 2; \qquad H_3 = 8x^3 - 12x; \qquad H_4 = 16x^4 - 48x^2 + 12$$

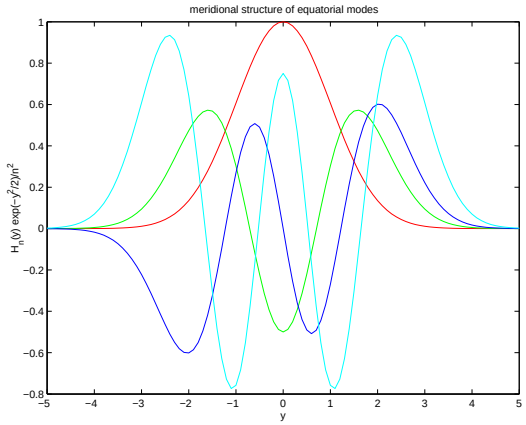

Figure 19: The latitudinal structure of the first few equatorial modes: $H_n(y)\exp(-y^2/2)/n^2$.

The dispersion relation is plotted in Fig. 20.

So, we have a complete set of waves, the Kelvin ($n = -1$), Yanai ($n = 0$), Rossby and Poincare ($n > 0$) waves. As seen in the plot, the dispersion relation includes two main sets of waves for $n > 0$. For high frequency, we can neglect the term $\frac{\beta k}{\omega}$, to find the Poincare gravity-inertial waves

$$\omega^2 \approx (2n+1)\beta c + k^2c^2,$$

while for low frequency, we can neglect the term ω^2/c^2 in the dispersion relation to find the westward propagating Rossby wave dispersion relation

$$\omega = \frac{-\beta k}{k^2 + (2n+1)\beta/c}.$$

Typical speeds of long Rossby waves would therefore be

$$\omega/k = \frac{-c}{2n+1}$$

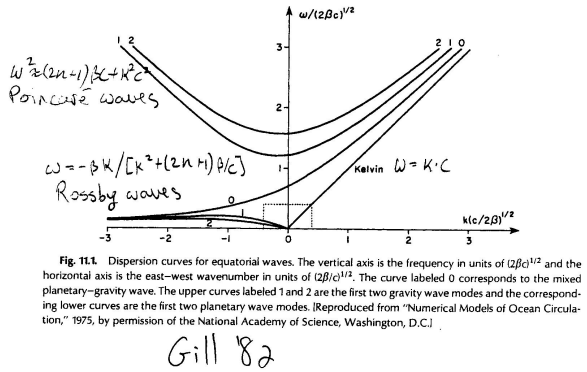

Fig. 11.1. Dispersion curves for equatorial waves. The vertical axis is the frequency in units of $(2\beta c)^{1/2}$ and the horizontal axis is the east–west wavenumber in units of $(2\beta/c)^{1/2}$. The curve labeled 0 corresponds to the mixed planetary–gravity wave. The upper curves labeled 1 and 2 are the first two gravity wave modes and the corresponding lower curves are the first two planetary wave modes. [Reproduced from "Numerical Models of Ocean Circulation," 1975, by permission of the National Academy of Science, Washington, D.C.]

Gill '82

Figure 20: The Equatorial wave dispersion relation, (Gill [20], p 438, Fig. 11.1)/

so that the first Rossby mode ($n = 1$) travels at a 1/3 of the Kelvin wave speed, implying a roughly 2.5 months crossing time for Kelvin and 8 months for Rossby waves (based on 15,000 km basin width).

Note (Fig. 19) that the first Rossby mode has a zero at the equator and two maxima away from the equator, while the Kelvin wave has a maximum at the equator. This tells us something about how a random initial perturbation will project on the different modes. That is, a forcing pattern or an initial perturbation that is centered at the equator may be expected to excite Kelvin waves, while a forcing or initial perturbation that has components off the equator will tend to excite Rossby waves. The above discussion centers on the first baroclinic mode, but may be generalized to higher vertical baroclinic modes, although for our purposes this is not essential.

1.2.4 Ocean response to wind perturbation

Consider first the mean state of the thermocline. The steady state ($\partial u/\partial t = 0$) momentum equation (1) in a reduced gravity model, at $y = 0$ ($\beta y v = 0$) in the presence of easterly wind forcing and neglecting frictional effects ($-\varepsilon u = 0$) is

$$0 \approx -g' \frac{\partial h}{\partial x} + \frac{\tau^x}{\rho_0 H}$$

so that an easterly wind stress is balanced by a pressure gradient due to a thermocline tilt, with the thermocline closer to the surface in the East Pacific. This mean state of the thermocline results in the cold tongue there, as observed, via the mixing of cold sub-thermocline water with the surface water, as will be discussed more quantitatively below.

Regarding the interannual equatorial thermocline variability, at this stage we just note that a wind perturbation that corresponds to a weakening of the mean easterlies in the central Pacific affects the thermocline depth in the central Pacific. It creates downwelling Kelvin waves (that is, waves that propagate a downwelling signal, which means a thermocline deepening signal; these are waves that propagate a warm water surplus above the thermocline, and may therefore be called "warm" waves) and upwelling (i.e. cold) Rossby waves. The excitation of these waves by a wind anomaly will be examined more rigorously below.

1.2.5 Atmospheric response to SST anomalies

We now need to describe the atmospheric response to SST perturbations. Use Gill's [19] model for this, whose equations are very much like the β plane ocean equations, except that the atmospheric time scales are much

shorter so that we assume the atmosphere to be in a steady state with the forcing by a specified heating Q,

$$-\beta yV = -\frac{\partial \Theta}{\partial x} - \varepsilon_a U \quad (5)$$

$$+\beta yU = -\frac{\partial \Theta}{\partial y} - \varepsilon_a V \quad (6)$$

$$c_a^2 \left(\frac{\partial U}{\partial x} + \frac{\partial V}{\partial y} \right) = -\varepsilon_a \Theta + Q. \quad (7)$$

where (U,V,Θ) stand for the zonal and meridional surface winds, and a geopotential ($dp = -g\rho dz = -\rho d\Theta$, Gill [20] section 6.17). The heating may be parameterized to be linear in the SST

$$Q = \alpha_T T.$$

We next need to use these equations to deduce the effect of an SST anomaly in the East Pacific on winds in the central Pacific. The above equations may be solved for a general heating function, and we only briefly outline the derivation of the solution (see Dijkstra, [9] p. 347). One first defines $S = \Theta + U$ and $R = \Theta - U$ and expands the heating and these two new variables in a series of parabolic cylinder equations, e.g.

$$Q(x,y,t) = \sum_{n=0}^{\infty} Q_n(x) D_n(y).$$

Next, these expansions are substituted into the Gill's model and equations are derived for $S_n(x)$ and $R_n(x)$ for each n. The solution of these equations for $n = 0,1,2$ is

$$\begin{aligned} R_0(x) &= \mu_0 \int_{x_w}^{x} e^{-\varepsilon_a (x-s)} Q_0(s) ds \\ R_1(x) &= 0 \\ R_2(x) &= \mu_0 \int_{x}^{x_e} e^{3\varepsilon_a (x-s)} (Q_2(s) + Q_0(s)) ds \end{aligned}$$

where $\mu_0 = \alpha_T \Delta T L / c_a^3$. Note that $R_0(x)$ is influenced by heating west of x, and thus represents the influence of atmospheric Kelvin waves that travel eastward, accumulate the influence of the heating, and thus influence the atmospheric state at x. The atmospheric Kelvin waves are damped (via the terms depending on ε_a) on their way, and therefore "remember" only the heating within a (nondimensional) distance $1/\varepsilon_a$ to the west of x. Similarly, $R_2(x)$ reflects the influence of atmospheric Rossby waves that travel westward toward x. In this case the waves travel slower, and thus by the time they arrive at x, they only "remember" the influence of the heating over a (nondimensional) distance of $1/(3\varepsilon_a)$.

Next, these solutions for R and S are transformed back to the physical variables U,V,Θ and truncated into the first 2-3 terms only in n, giving

$$U(x,y=0) = \frac{3}{2} R_2(x) - \frac{1}{2} R_0(x)$$

Finally, we assume that the atmospheric heating occurs only over the east Pacific

$$Q(x) = \alpha_T \delta(x - x_e) T(x_e)$$

and perform the integrations over x in the above expressions for $R_{0,1,2}$ to find that only the atmospheric Rossby wave solution that propagates from x_e to x affects the wind speed at x

$$U(x,y) \propto -e^{(x-x_e)/(c_a/3\varepsilon_a)} T(x_e) e^{-\frac{1}{2}y^2/(L_R^a)^2} \quad (8)$$

where $c_a \approx 40 m/sec$; $\beta = 2.3 \times 10^{-13} cm^{-1} sec^{-1}$; $L_r^a = \sqrt{2c_a/\beta} \approx 2 \times 10^3 km$, and the decay scale of the influence of the east Pacific heating on the zonal wind west of that point is $(c_a/3\varepsilon_a) \approx 3500 km$ for $\varepsilon_a \approx 3 day^{-1}$.

1.2.6 On the atmospheric heating

As a simple entry point to this subject, it is convenient to consider the atmospheric heating parameterization used in intermediate El Nino models such as the Cane-Zebiak [66] model. This parameterization assumes that the anomalous atmospheric heating is dominated by diabatic heating that occurs via latent heat release due to moisture condensation. The heating is divided into a contribution due to condensation of water evaporated locally at the ocean surface (Q_s) and another contribution due to the condensation of the larger scale humidity field induced by upward air motion that results from a local wind convergence (Q_1),

$$\begin{aligned} Q &= Q_s + Q_1 \\ Q_s &= (\alpha T)\exp[(\overline{T} - 30^\circ C)/16.7^\circ C] \\ Q_1 &= \beta_*[M(\overline{c}+c) - M(\overline{c})] \\ c &= -[U_x + V_y]. \end{aligned}$$

The function $M(x)$ is defined as

$$M(x) = \begin{cases} x & x > 0 \\ 0 & x \leq 0 \end{cases}$$

The local evaporation parameterization is simply an empirical curve fitting of the Clausius-Clapeyron relation + linearization which together give the saturation vapor pressure (pressure at which vapor and liquid water can coexist) at a temperature T

$$q_w(\overline{T} + \delta T) = a\exp[-\frac{b}{T+\delta T}] \propto \delta T \exp[-\frac{b}{T}]$$

The dependence of the atmospheric heating on the mean SST, $\overline{T}$, is therefore exponential, hence quite strong. The increase in climatological monthly equatorial eastern Pacific mean SST from about 23°C in September to about 26.5°C in March-April corresponds to a 25% enhancement in the perturbation heating Q_s for the same SST perturbation.

The condensation of the larger scale humidity field due to the local wind convergence is again influenced by the mean conditions; in this case the mean convergence: only if the total convergence $\overline{c}+c$ is positive, is the local air motion upward. And only if the local motion is upward, does it induce condensation and therefore atmospheric heating. The mean convergence in the east equatorial Pacific is determined by the seasonal location of the ITCZ. When the ITCZ is near the equator, the mean convergence is positive, and anomalous atmospheric convergence is effective in causing atmospheric heating. When the ITCZ is away from the equator, the mean convergence is negative, and anomalous convergence does not cause diabatic heating.

Overall, it is important to note that the response of the atmospheric heating to a given SST anomaly depends on the mean atmospheric conditions which vary seasonally. As we shall see below, this dependence on the mean seasonal conditions introduces some interesting dynamical effects.